



## Combining CFD and Experimental Approaches to Optimize a Spray Release in a 20 L Sphere

Pierre Chot-Plassot<sup>a</sup>, Alexis Vignes<sup>a,\*</sup>, Carlos Murillo<sup>a</sup>, Jean-Marc Lacome<sup>a</sup>,  
 Stephanie El-Zahlanieh<sup>a,b</sup>, Nathalie Bardin-Monnier<sup>b</sup>, Olivier Dufaud<sup>b</sup>

<sup>a</sup>INERIS, Parc Technologique ALATA, BP 2, F-60550, Verneuil-en-Halatte, France

<sup>b</sup>Université de Lorraine, CNRS, LRGP, F-54000 Nancy, France

[alexis.vignes@ineris.fr](mailto:alexis.vignes@ineris.fr)

European regulations require that the risk of an explosive atmosphere (ATEX) associated with the production of a flammable mist be assessed. In order to properly investigate mist flammability, a dedicated experimental tool was developed based on the standardized 20L explosion sphere and an additional Venturi injection system. As part of its design, the conditions of mist generation must be fully controlled. To complement the experimental approach, a computational fluid dynamic modeling (CFD) has been developed with an Euler-Lagrange method. It aimed at determining the homogeneity of the mist and the influence of the turbulence on the droplet size distribution (coalescence / fragmentation dynamics) as it greatly influences the mechanism of combustion. Based on previous studies and on industrial considerations, ethanol and kerosene were chosen. Modeling results were compared to the droplet size distribution determined by laser in-situ measurements and to the flow characteristics measured by particle image velocimetry. The CFD modeling confirmed the significant effect of the turbulence on the droplets coalescence and enabled to improve the understanding of the phenomenology related to the dispersion of a flammable mist into a 20L sphere. These results are consistent with the droplet particle distributions measured experimentally and show that CFD modeling can support further experimental developments so that it can constitute the basis for a new standard 20L explosion sphere for mists testing.

### 1. Introduction

European regulations require an assessment of the explosive atmosphere (ATEX) risk associated with the production of a flammable aerosol (e.g. diesel, lube oil, gasoline mists). However, such a risk analysis is sometimes difficult due to the lack of tools to correlate dispersion conditions with their flammability and there is no standard for the experimental determination of the ignition sensitivity or explosion severity of a mist.

The specifications for a new standard must include the availability of test equipment, its ease of use and both its specific and versatile nature. Therefore, a new experimental set-up was developed based on the classic 20L explosion sphere, already conventionally used to determine the explosion severity of gases and dusts. However, mists do not, of course, have the same properties and behavior as powders or gases: unlike gases, their dispersion in the air is not stable over time; unlike powders, droplets are subject to coalescence and can be captured onto the sphere wall (rain-out phenomenon). Their properties and specificities imply some modifications of the set-up and adaptation of the test procedures.

In order to describe the dispersion of a flammable spray in the modified 20L explosion sphere and to determine the most conservative or representative test conditions, experimental characterizations have been performed using i) particle image velocimetry to study the turbulence of the mist, ii) laser in-situ measurements for the determination of the droplet size determination, iii) high-speed videos, to observe the homogeneity and stability of the suspension. Preliminary tests were performed on various hydrocarbons, such as kerosene JetA1, diesel, ethanol, biodiesel or light fuel oil. Nevertheless, as extensive as it may be, this experimental study cannot cover all possible configurations because the influential parameters (type of ejection nozzle, diameter, temperature, injection pressure, nature of the fluid, etc.) and their combinations are too numerous.

In this context, a computational fluid dynamic modeling (CFD) has been developed with an Euler-Lagrange approach to analyze the biphasic flow development inside the test apparatus and assess the flow conditions pertaining to the fragmentation and the coalescence of the dispersed phase. After adjusting the CFD simulation to the design specifications of the apparatus, CFD simulations were used to investigate the local concentration in the 20L explosion sphere beyond the experimental observations to predict the droplet size distribution, the mist homogeneity and the time-evolution of the local concentration near the ignition source.

## 2. Experimental set-up and CFD modeling

The experimental set-up will be briefly described as well as the models applied in the CFD approach.

### 2.1 The modified 20L sphere for mists testing

The experimental set-up was described by El - Zahlanieh et al. (2022). It consists of a standard 20L explosion sphere, whose dust container and outlet valve have been removed and replaced by a Venturi system connected at the bottom of the sphere. The mist is dispersed by the injection of an air-liquid mixture at a high pressure through an injection nozzle. Various injection sets of different diameters are available. Two electronic valves allow the control of the inlet flow rates and the air/liquid ratio. Before injecting the air/fuel mixture, a partial vacuum is created in the sphere at a calculated pressure depending on the mist concentration to be attained. When the mist has been completely injected, the pressure inside the sphere is equal to the atmospheric pressure. An ignition system (spark or chemical igniter) allows the combustion of the hydrocarbon mist. In addition to the nature of the fluid, the mass injected, the injection time and pressure, the nozzle type and diameter can be varied to change both the mist concentration and droplet size distribution. Tests were notably performed on ethanol, kerosene, isooctane, lube oil and biodiesel. This study will be limited to kerosene JetA1, with a single experimental configuration ('N1' nozzle) and an injection pressure of 3 bar.

### 2.2 Experimental characterization of JetA1 mists

Some variables were characterized experimentally in order to both feed and validate the numerical approach. The droplet size distribution (DSD) was determined in situ (at the center of the 20L sphere) using a laser sensor (Helos from Sympatec) on a 0.5 - 175  $\mu\text{m}$  range at a frequency of up to 2000 Hz. Unfortunately, the analysis duration is limited to 5 s due to the rain out phenomenon occurring on the glass walls. The droplet size distribution obtained with a 'N1' nozzle is rather stable over time and can be represented by the characteristic diameters shown in Table 1. It should be noted that, by using other injection nozzles, mean droplet diameter up to 80  $\mu\text{m}$  can be obtained. An average flow rate of  $2.5 \cdot 10^{-4}$  kg/s was measured for the liquid phase, which represents from 17 to 33 wt% of the biphasic flow. Particle image velocimetry (PIV) was implemented to study the time evolution of the droplet velocity and of the root-mean-square velocity ( $v_{\text{rms}}$ ) of the flow. Velocity magnitudes  $v$  ranging from 0.5 to 15 m/s were attained at the sphere center during the mist generation, with a maximum  $v_{\text{rms}}$  of 2 m/s at the end of the liquid injection.

Table 1: Characteristic diameters of JetA1 mists generated in the 20L sphere

| Diameters ( $\mu\text{m}$ ) | $d_{10}$ | $d_{50}$ | $d_{90}$ | $d_{99}$ | $d_{3,2}$ |
|-----------------------------|----------|----------|----------|----------|-----------|
| Kerosene JetA1              | 5.5      | 7.3      | 10.6     | 13.7     | 7.3       |

### 2.3 Dimensionless numbers related to mist generation and CFD theoretical approach

Using the experimental parameters presented in section 2.2 and the fluid properties, a set of dimensionless numbers of interest for this study was evaluated (Table 2). A study in the duct connecting the air tank and the nozzle was carried out on the PHAST software. This resulted in an outlet velocity at the orifice equal to 313 m/s which will be considered here. For these dimensionless calculations only, the droplet size distribution was assumed monomodal and equal to the mean diameter  $d_{50}$ . According to the values of the dimensionless numbers represented in Table 2, the spray is qualified as fine (volume fraction lower than 1 %). However, the use of a four-way coupling is still necessary because the jet is confined, the flow is highly turbulent and droplet-droplet interactions cannot be neglected. As expected, Weber number is greater than 350 (Pilch, 1987) and Ohnesorge number is less than 1 (Kadesh, 2020), which means that a catastrophic breakup of the droplets occurs when they exit the nozzle (fragmentation). The droplets follow the air trajectory ( $St < 1$ ) and a collisional regime is assumed ( $Kn < 1$ ) because the experiment showed collisions between the droplets. Jet was atomized at 95% at the orifice. An Euler-Lagrangian solver was then chosen to model the droplets and gas phase. The simulations were done using OpenFoam v1912. The dimensionless numbers detailed hereafter were used to select the most suitable solver: SprayFoam solver was chosen because it takes into account fragmentation and allows modeling the evolution of the droplet sizes distribution. It considers the fragmentation and the collision of

the droplets. It should be noted that the wall-droplet interactions within the sphere was not considered in this preliminary modeling study. Wall-droplet interactions were then configured so that the droplets stick to the wall (Table 3). The turbulence models used are of the RANS type, i.e. only the large scales of the turbulence will be solved numerically while the small and medium scales will be modeled. Regarding the high Re and the confined environment, the k- $\omega$  sst model was implemented. It consists in applying the classical k- $\epsilon$  model far from the walls and the k- $\omega$  model close to the wall (Table 3).

*Table 2: Characteristic dimensionless numbers for the generation of a JetA1 mist in the 20L sphere at the injection orifice*

| Dimensionless number | Vol. fraction | Re <sub>air</sub> | We    | Oh   | St                   | Kn  |
|----------------------|---------------|-------------------|-------|------|----------------------|-----|
| Value (-)            | 0.02 %        | 52000             | 21500 | 0.13 | 2.4.10 <sup>-4</sup> | < 1 |

The turbulence models used are of the RANS type, i.e. only the large scales of the turbulence will be solved numerically while the small and medium scales will be modelled. Regarding the high Re and the confined environment, the k- $\omega$  sst model was implemented. It consists in applying the classical k- $\epsilon$  model far from the walls and the k- $\omega$  model close to the wall (Table 3). O'Rourke's model was chosen to represent the collision between two droplets (Table 3). It is based on a statistical approach and assumes that two droplets can only collide if they are in the same cell. Therefore, the result of a collision can be a coalescence, if the droplets collide head-on, or a rebound, for an oblique collision.

*Table 3: Theoretical models used for CFD modeling of a JetA1 mist in the 20L sphere*

| Phenomena | Forces                 | Turbulence                           | DSD               | Fragmentatio<br>n | Heat transfer | Collision | Interactions                 |
|-----------|------------------------|--------------------------------------|-------------------|-------------------|---------------|-----------|------------------------------|
| Models    | Gravity,<br>drag force | k- $\epsilon$ and<br>k- $\omega$ sst | Rosin-<br>Rammler | Reitz-<br>Diwakar | Ranz-Marshall | O'Rourke  | Standard Wall<br>Interaction |

## 2.4 Setup of the CFD modeling

The kerosene spray is considered as a two-phase jet in a confined, compressible, unstable and turbulent environment. Modeling and meshing were done on Ansys v2021 (Design Modeler and Meshing) (Figure 1). An optimal mesh size is based on a good quality of orthogonality of the meshes. A cartesian cut-cell mesh (CutCell) was chosen and a refinement was made near the injection (Figure 1b) and at the center of the sphere (Figures 1.c) and d) in order to obtain accurate results. The quality of orthogonality is 98% and the number of meshes is set at 500,000.

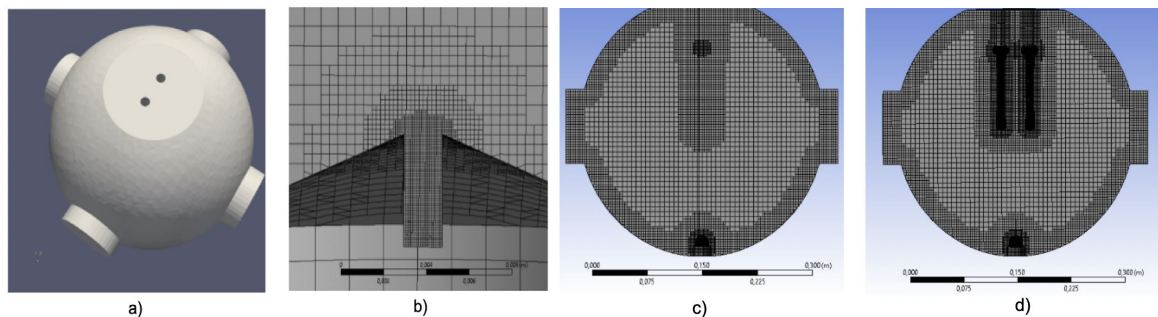


*Figure 1: 20 L explosion sphere modelled and meshed with the CutCell meshing algorithm. a) global view, b) focus on the injection zone, c) lateral view 1 and d) lateral view 2*

The dimensions of the 'N1' orifice are of the order of  $1.8 \cdot 10^{-3} \times 5.8 \cdot 10^{-4} \text{ m}^2$ . In order to obtain a sufficient accuracy, at least six meshes per dimension must be placed in this area, which implies a mesh size of approximately  $1 \cdot 10^{-4} \text{ m}$ . The simulation is done by a Crank-Nicholson semi-implicit time scheme. Spatial schemes were chosen according to the mesh orthogonality and to a lesser numerical diffusion. The time step  $dt$  is calculated with respect to the smallest mesh of the geometry. By definition, the stability criterion (CFL) is equal to 1; beyond that value, the stability and accuracy of the results are significantly reduced:

$$CFL = \frac{v \cdot dt}{dx} \quad (1)$$

This implies that a time step equals  $3 \cdot 10^{-7}$ , which is too costly in terms of computing time. It was decided to increase the time step to  $1.5 \cdot 10^{-5} \text{ s}$ , therefore the corresponding CFL value is much higher. Iterative procedure

was achieved with solver factors to obtain the best compromise between stability and accuracy. The mist injection was represented by fluid parcels containing several droplets of the same physical size in order to reduce their number and keep the same mass of injected liquid constant.  $10^5$  parcels per second containing an average of 10000 droplets has been configured following a sensitivity analysis, which aimed at determining the adequate calculation time to represent liquid mass flowrate reliably. A system of ordinary differential equations is solved to predict mass, velocity and temperature evolutions. The droplets were assumed to be spherical. Mass flow rate of gas and liquid are set to  $4.9 \cdot 10^{-4}$  kg/s and  $2.5 \cdot 10^{-4}$  kg/s respectively.

### 3. Results and discussion

CFD simulations were validated using the experimental results presented in section 2.2. Then, the hydrodynamics of the mist and the time-evolution of its droplet size distribution (coalescence/fragmentation) was studied. It should be stressed that the knowledge of the DSD at the center of the sphere (ignitor location) is crucial to better understand the mist combustion mechanism.

#### 3.1 Analysis of spray velocity iso-contour lines

Figure 2 shows the velocity vector during mist generation, from 300 to 1500 ms on a slice set up at the sphere center (velocity magnitude  $u$  in m/s).

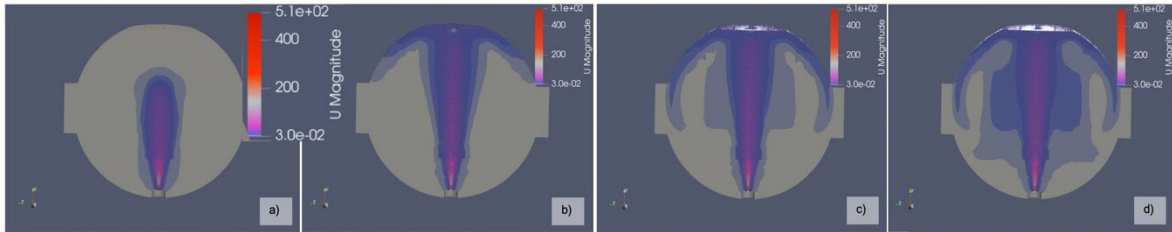


Figure 2: Time-evolution of the jet velocity in the sphere at a) 300 ms, b) 500 ms, c) 1100 ms and d) 1500 ms

The fluid ejected from the nozzle disperses vertically in a cone and then hits the upper part of the sphere at around 400 ms (Figure 2b). Once the mist contacts the walls, recirculation zones are formed in the middle of the sphere (Figure 3). In the middle of the sphere, the turbulent kinetic energy  $k$  (velocity fluctuation) as well as the velocity is high.

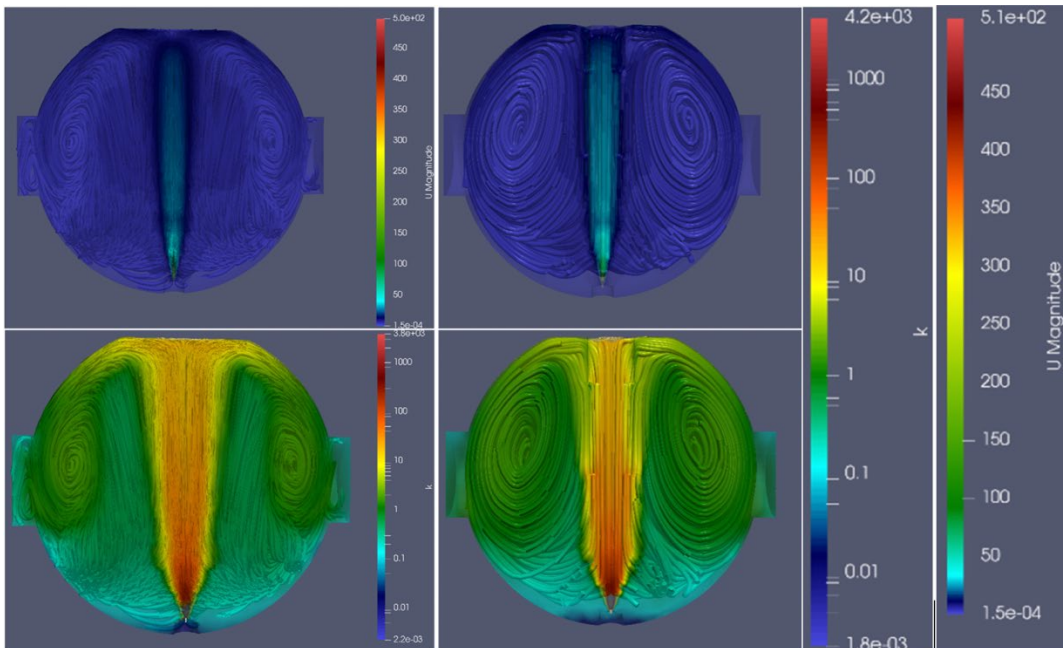


Figure 3: Representation of streamlines and iso-contour lines of a) velocity in lateral view 1, b) velocity in lateral view 2, c) turbulent kinetic energy in lateral view 1 and b) turbulent kinetic energy in lateral view 2.

Figure 4 shows the temperature iso-contour lines at the orifice. It was found that a) the temperature decreases up to  $-75^{\circ}\text{C}$  within the expansion zone and then increases to the initial temperature of  $20^{\circ}\text{C}$ ; b) the jet accelerates from  $390\text{ m/s}$  at the nozzle exit to  $510\text{ m/s}$  in the expansion zone and then slows down to a velocity close to  $1\text{ m/s}$ . The cooling down effect and the speed up in velocity are explained by the expansion of the supersonic air jet. The velocities obtained by CFD and PHAST are of the same order of magnitude. The decrease of the CFL stability criterion could enable to obtain more accurate results.

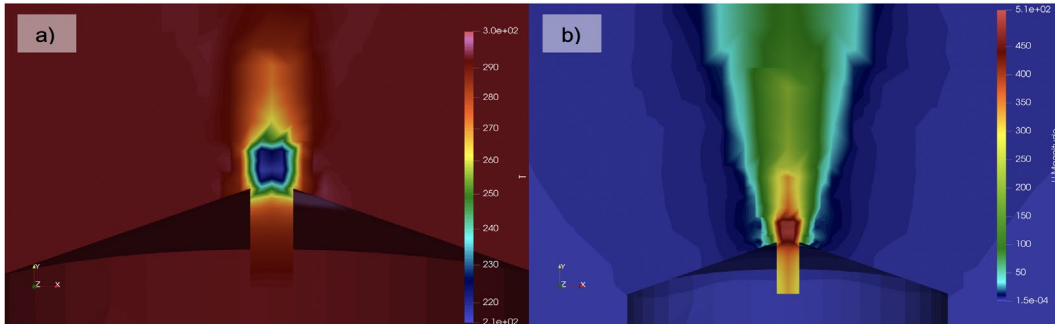


Figure 4: Representation of a) temperature and b) velocity iso-contour lines at the nozzle

### 3.2 Time and spatial evolution of the droplet size distribution

In order to implement this preliminary CFD modeling study, the initial DSD at the orifice was taken equal to the experimental DSD at the center of the sphere at  $t=1\text{ s}$ , keeping in mind that the DSD at the orifice cannot be observed experimentally. In the future, the initial DSD will be adapted to reach experimental DSD at the center of the sphere. Meanwhile, this current study is a first step to investigate the main phenomena and to validate the consistency of the approach. In order to observe by CFD modeling the evolution of the droplet size and velocity distribution, a block was modelled in Paraview at the center of the sphere to capture the droplets passing through this volume. The droplet size distribution at the center of the sphere is shown in Figure 5. The shape of the DSD obtained by CFD modeling looks like the experimental DSD obtained in the center of the sphere at  $t=1.5\text{ s}$  (Figure 5). However, the mean diameter of the numerical DSD ( $4.5\text{ }\mu\text{m}$ ) is lower than the mean diameter of the experimental DSD ( $7.5\text{ }\mu\text{m}$ ). The initial DSD at the orifice will then require to be modified by increasing the mean diameter of the droplets. It should be also noted that, due to the choice of the collision model (O'Rourke – Table 3,) c) Further mesh refinements will be tested in order to ensure that coalescence collisions is well represented in the CFD modeling compared to the experimental reality (Pischke, 2014). Furthermore, it has been observed previously existence of recirculation zones (turbulence) in the center of the sphere. This aspect is all the more important that a strong correlation exists between turbulence and coalescence/fragmentation which influences the combustion mechanism.

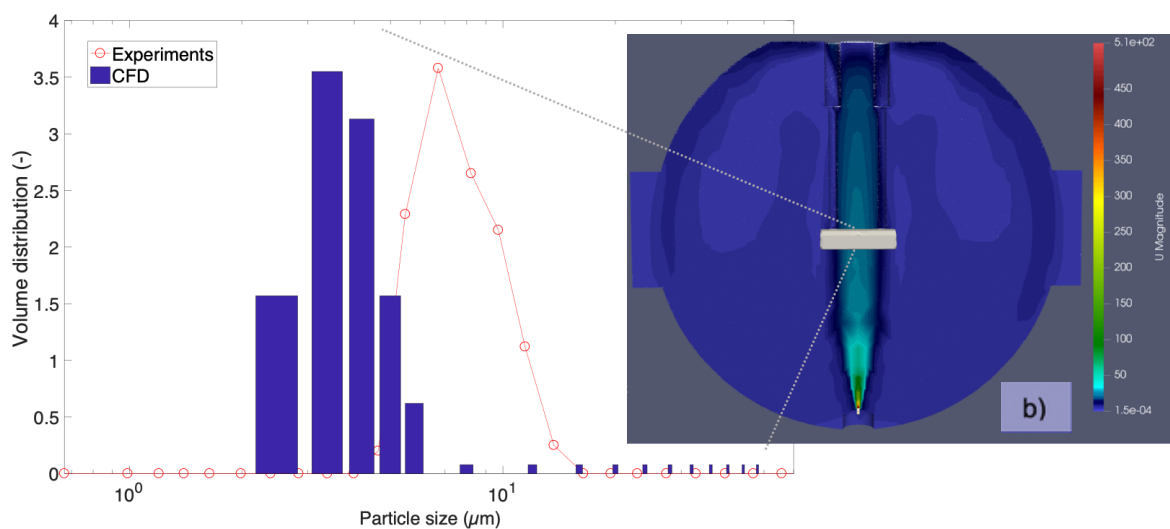


Figure 5: Comparison between CFD results and the experimental kerosene DSD at the sphere center after  $1.5\text{ s}$  generation

The mesh size will be adapted in a near future to refine the results and better discriminate the phenomena of collision, evaporation and fragmentation.

#### 4. Conclusions

The work carried out made it possible to study the phenomenology related to the dispersion of a non-flammable fog in a 20 L explosion sphere and to investigate the behavior of the fuel dispersion. In the course of this study, an overview of liquid and diphasic free air jets was presented to introduce the experimental study carried out. This study modelled and simulated a supersonic spray of air and kerosene in a 20L closed sphere using Ansys meshing and Openfoam. The flow was solved by an Eulerian-Lagrangian method and the equations were discretized temporally in semi-implicit by the Crank-Nicholson scheme. A dimensionless study of Reynolds, Stokes, Knudsen, Ohnesorge, Weber numbers based on the experimental observations at the centre of the device were used to set up the input data for the CFD simulation. A CFD calibration strategy on the experimental model and the development of the CFD configuration were described. The numerical results showed the impact of turbulence on the droplet size distribution (coalescence/fragmentation). Strong turbulence and recirculation zones in the middle of the 20L sphere were observed to influence droplet size through coalescence and fragmentation phenomena. These results will support experimental investigations on the combustion of mist droplets as it is directly under the influence of the DSD and turbulence. Further investigations are also foreseen to explore rain-out (droplets-wall interactions) phenomenon than can lead to the formation of a layer of liquid on the walls of the 20L sphere which may influence the explosion severity of the mist by changing locally vapor concentrations.

#### Acknowledgments

This work was supported financially by the French Ministry for the Ecological and Solidary Transition and The French Ministry for Higher Education and Research.

#### References

- El - Zahlanieh S., Sivabalan S., Dos Santos I.S., Tribouilloy B., Brunello D., Vignes A., Dufaud O., 2022, A step toward lifting the fog off mist explosions: Comparative study of three fuels, *Journal of Loss Prevention in the Process Industries*, 74, art. no. 104656.
- Pilch M., Erdman C.A., 1987, Use of breakup time data and velocity history data to predict the maximum size of stable fragments for acceleration-induced breakup of a liquid drop, *International Journal of Multiphase Flow*, 13, 6, 741-757.
- Kadem N., 2005, Atomization of an irrigation gun jet: Eulerian modeling and validation (In French: Atomisation du jet d'un canon d'irrigation: modélisation eulérienne et validation, Phd Thesis, University of Marseille II, Marseille, France.
- Pischke Ph., Kneera R., Schmidt D.P., 2015, A comparative validation of concepts for collision algorithms for stochastic particle tracking, *Computer and Fluids*, 113, 77-86.